Friction modelling and simulation at system level - Considerations to load and temperature effects

Jean-Charles Maré

Friction modelling and simulation at system level: Considerations to load and temperature effects

Jean-Charles Maré

The influence of load and temperature on friction is addressed in a practical way to provide a step forward in simulation-based design through the development and the numerical implementation of realistic system-level models of frictional losses. Hydraulically and electrically supplied actuators are considered at both individual component level (e.g. gear pairs, nut–screws or bearings) and integrated equipment level (e.g. reducers or even complete actuators). The need for more realistic modelling of friction for embedded and more electrical systems is highlighted, and the influence of load and temperature is illustrated from measurements. The state of the art is reviewed considering knowledge models with special focus on physical effects and data commonly supplied by components' manufacturers. Then, special attention is paid to global representation models developed as a parameterized combination of generic friction effects, and a generic framework for introducing load and temperature effects in system-level friction models is proposed. Candidate options for model structure, parameterization, numerical implementation and inverse simulation are discussed. The last part of this article supports the development of friction models from mechanical efficiency data, the parameter most widely handled by designers and suppliers, with special attention to aiding or opposite load and to sticking. Throughout this arti-cle, measured friction forces are extensively reported and compared with the proposed models.

Keywords
Actuator, efficiency, electromechanical, fluid power, friction, load, modelling, simulation, system, temperature

Introduction

Simulation-based design is continuously attempting to broaden its scope in order to accelerate the development phase while reducing technical risks. Therefore, reproducing friction losses in a realistic way for sizing and for virtual prototyping has recently become a challenging issue for the designer willing to take a holistic view when addressing the following:

Energy consumption over typical missions, for greener designs offering more environment-friendly and cheaper operation, for example, with regenerative architectures.
Steady-state and transient power variables (e.g. forces, currents, volume flow), for more accurate power sizing and lifetime/reliability prediction at component and system levels.
Peak power demand in power networks, for energy storage, power spike filtering and optimization of power network architecture and management.
Thermal balance, to enable downsizing of components while keeping local temperature consistent with lifetime/reliability requirements.

This particularly applies to the more electrical power drives that are progressively tending to replace fluid power ones, for example, for embedded actuation systems in aerospace.[1] When attempts to save mass and energy are considered, this situation raises two main issues that require step changes in engineering practices.

First, in hydraulic drives, hydrostatic power is transmitted by means of mass transfer. Although this mass transfer induces severe design and operating constraints

Institut National des Sciences Appliquées, Université de Toulouse, INSA, UPS, Mines Albi, ISAE, ICA (Institut Clément Ader), Toulouse, France

Corresponding author:
Jean-Charles Maré, INSA Département de Génie, Mécanique, 135 Avenue de Rangueil, 31077 Toulouse, Cedex 4, France.
Email: jean-charles.mare@insa-toulouse.fr

(fluid expansion and leakage compensation, filtering and bleeding, integration of power distribution pipes), it has a real advantage as far as heat transfer is concerned: the heat generated by energy losses at actuator level is 'naturally' evacuated by the fluid flowing to the reservoir through the return line. In this situation, the hydraulic fluid also plays the role of a heat conveyor, thus eliminating thermal issues at actuator level. In electrical power drives, power is transmitted without any mass transfer. Therefore, the thermal balance of electrically powered actuators often becomes a major design driver for sizing.[2] Any frictional force in the power path between motor and load will generate heat. Through a snowball effect, this will require additional driving torque from the motor, which will have to be fed by higher currents. In their turn, these currents will increase the copper losses in motor windings and the conduction losses in the electronic power drive.

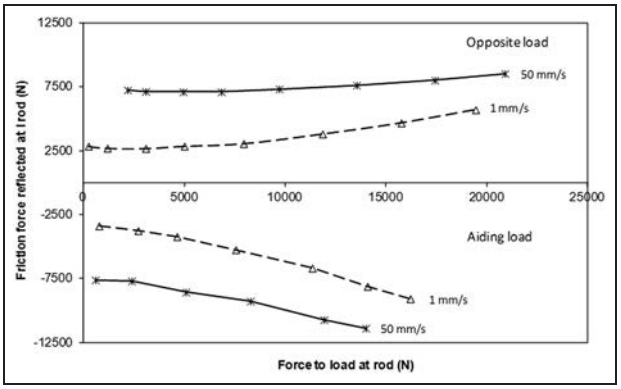

Figure 1. Measured friction force reflected at rod level for a roller screw in a direct-drive electromechanical actuator.

Second, in the switch from hydraulic to electric drives, another effect requires the development of more representative friction models. Instead of being driven by pressure pulses and the travel distance of high-pressure seals, service life and reliability are impacted by the sizing of rolling (or even sliding) mechanical elements such as gears, ball or roller screws, bearings and joints. In this situation, the sizing activity requires the calculation of mean values from the load forces and velocity during a typical mission. When power needs are propagated from load to power source through inverse simulation, any friction loss can significantly impact the sizing of the components located upstream in the functional power path.

Over the last few decades, the modelling and simulation of friction have been widely and deeply investigated for the design of power transmissions. Virtual prototypes have mainly been developed to support control design where obtaining a realistic representation of friction forces is an essential step towards accurate prediction of closed-loop performance. Most of the models principally consider the non-linear dependence of friction on velocity, as reviewed in Maré.[3] This is a logical extension from the control designer's point of view, in which a pure viscous friction model is used for linear analysis and control needs by assuming the friction force to be simply proportional to the relative velocity. However, the influence of load and temperature on friction forces has generally been set aside, even though it can play a greater role than velocity does. This is illustrated in Figures 1 and 2. Figure 1 shows the influence of load on friction in an inverted preloaded roller screw, direct-drive electromechanical actuator (EMA) (lead 3 mm, rated force 50 kN, preload 3 kN).[4] The measured frictional force reflected at the rod side is plotted as a function of the

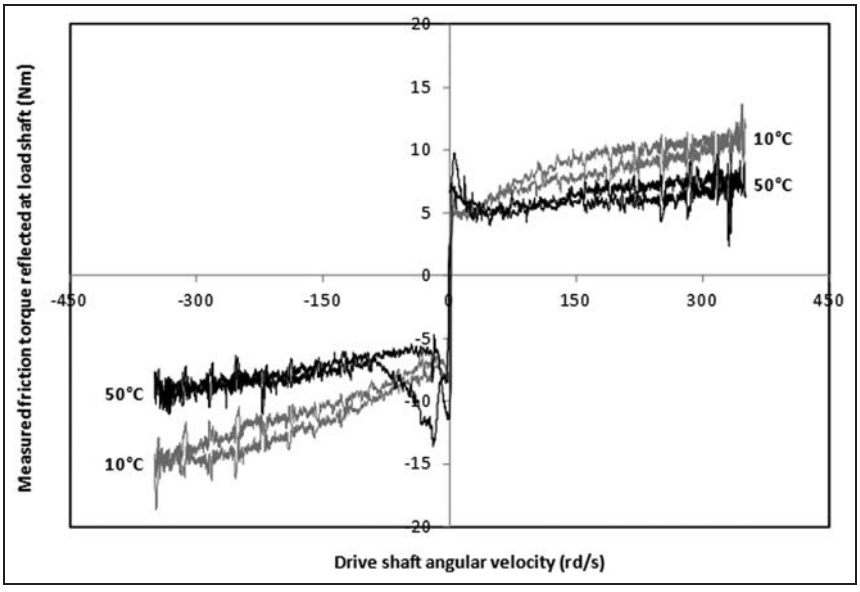

Figure 2. Measured friction torque reflected at output shaft for Harmonic Drive® CPU-32-50-M reducer with standard grease (20 N m torque to load).

screw angular velocity and the load force at rod end. It can be observed that for a given velocity, the magnitude of the frictional force can vary by a factor of 3 with respect to the load.

The influence of temperature is illustrated in Figure 2 for a Harmonic Drive® (HD) epicyclic reducer (ratio 50, rated output torque 216 N m).[5] The measured friction torque reflected at the output shaft is plotted at 10% load torque, as a function of the driving shaft velocity for different operating temperatures. As frequently reported, sensitivity to velocity clearly appears as a combination of Coulomb, viscous and Stribeck effects. Less commonly mentioned is the significant dependency of the last two effects on temperature, even for a 40 °C change.

Both figures show that load and temperature may influence friction in the same order of magnitude as the velocity does, especially under aiding load conditions. Moreover, these two plots highlight the presence of another effect that is generally neglected: the power quadrant effect. As can be observed, the amount of friction is very sensitive to the quadrant of operation, whether power flows from functional power source to load (opposite load) or from load to power source (aiding load).

However, it is surprising to note that most published works only consider the friction dependence on velocity, while very few introduce the load and temperature effects in friction models, although they may play a major role. This situation motivated the development of more realistic friction models for the preliminary sizing and virtual prototyping of embedded power transmission systems, in particular at the author's laboratory. Most of the model development was driven by a mixed approach, considered to be a judicious combination of physical models and representation models suggested by experimental data.

System-level modelling of integrated devices like actuators or even gearboxes may be performed using either a bottom-up or a top-down view. The first concerns more virtual integration of component models to make an equipment-item model. The second is more related to development activities where no detailed data are available on the internal structure and the parameters of the device under study: the equipment is modelled globally without considering the factors contributing to friction losses. The first section below reviews the state of the art in modelling friction losses for the definition of mechanical power transmission components and analyses the associated friction data that are commonly supplied by components' manufacturers. The second section focuses on the details of the introduction of load and temperature effects in friction representation models for actuation equipment, considering both hydraulic and mechanical devices. Accordingly, a generic framework for friction models, including load and temperature effects, is proposed in the third section, paying special attention to model structure, parameterization, numerical implementation and inversion. As mechanical efficiency is widely employed for sizing, the last section is dedicated to linking friction forces to mechanical efficiency and thus to ensuring continuity between sizing and virtual prototyping activities. The associated process is detailed with care to represent the quadrant effect and sticking in a realistic way.

State of the art

In the field of actuation, there are a variety of sources of information that can serve friction modelling at system level. The first ones generally concern component sizing or selection: knowledge models are obtained from theoretical developments in applied mechanics, while numerical data are provided by component or equipment suppliers. Another important source is to be found more from control design and virtual prototyping and provides representation models that aim to reproduce the observed effects without particular consideration of the underlying physics. Standards and recommendations issued by institutes and associations (e.g. International Organization for Standardization (ISO), American Gear Manufacturers Association (AGMA), American National Standards Institute (ANSI)) may also be of interest.

Knowledge models

Power transformers. Mechanical power transformers transmit forces through contacts between solids with rolling effects (e.g. roller- or ball screws), sliding effects (e.g. worm gear) or mixed effects (e.g. gear pairs). Mechanical efficiency can be calculated formally from the geometry of the facing pieces and from the basic friction model at contact. Sliding losses are generally dominant for low-speed/high-force operation. Besides load-dependent losses, churning, windage and seals may add significant frictional losses. Unfortunately, these load-independent mechanical losses are strongly influenced by integration and lubrication (type and realization). For this reason, it seems difficult to establish a generic model, as pointed out in recent reviews.[6–8]

Table 1 summarizes the models of mechanical efficiency in a synthetic form for the most common types of mechanical power transformers. It can be noted that

- For nut–screws, the simplified expression is extensively used because the friction factor and the helix angle are generally low.
- For spur gears, the common Shipley model mentioned in Dudley and Townsend[9] gives the average specific sliding along the contact path from extreme values. A more recent study[10] improves the model of Anderson and Loewenthal[12] by using a validated representation model of the friction term.
- There is no mention of the indirect efficiency of spur gears.

Table 1. Summary of efficiency models for mechanical power transformers.

	Efficiency	Remarks
Nut–screw		
Exact	$\eta_d = \frac{\tan(\beta)}{\tan(\beta+\varphi)} \approx \frac{1}{1+\mu/\beta}$ $\eta_i = \frac{\tan(\beta-\varphi)}{\tan(\beta)} \approx 1-\mu/\beta$ $\eta_p = \frac{\tan(\beta)}{\tan(\beta-\varphi)} \approx \frac{1}{\mu/\beta-1}$	β helix angle $\beta = p/\pi d$ $\varphi = \arctan(\mu)$ p pitch, d screw diameter, μ friction factor Simplified when $\tan(u) \approx u$, error lower than 1% for $u = 10°$
Spur gear (external, no shift, no correction)		
Townsend model[9]	$\eta_d = 1 - \frac{\mu}{2\cos(\alpha)} \frac{(H_s^2+H_t^2)}{H_s+H_t}$ with $H_s = (R+1)\left[\sqrt{\left(\frac{D_a}{D}\right)^2 - \cos^2\alpha} - \sin\alpha\right]$	α pressure angle a center distance D, d pitch diameter of gear and pinion R reducer ratio, $R = D/d$ m module D_a, d_a outside diameters of gear and pinion $D_a = D + 2m$, $d_a = d + 2m$ H_t specific sliding at start of approach action H_s specific sliding at end of recess action
Pleguezuelos model[10]	$\eta_d = 1 - 2\pi\left(\frac{1}{z}+\frac{1}{Z}\right) f_{rm}$ with $f_{rm} = c_0\mu + c_1\mu\varepsilon_\alpha + c_2\mu\varepsilon_\alpha^2$ $\varepsilon_\alpha = \frac{\sqrt{\left(\frac{d_a}{2}\right)^2 - \left(\frac{d_b}{2}\right)^2} + \sqrt{\left(\frac{D_a}{2}\right)^2 - \left(\frac{D_b}{2}\right)^2} - a\sin\alpha}{\pi m\cos\alpha}$	Z, z, number of teeth on gear and pinion $Z = D/m$, $z = d/m$ ε_α transverse contact ratio D_b, d_b base diameters of gear and pinion $D_b = D\cos\alpha$, $d_b = d\cos\alpha$ For $1 < \varepsilon_\alpha < 2$, $c_0 = 0.1464$, $c_1 = -0.1201$, $c_2 = 0.1327$ For $2 < \varepsilon_\alpha < 3$, $c_0 = -0.0620$, $c_1 = -0.2224$, $c_2 = 0$
Worm gear Kohara[11]	$\eta_d = \frac{\cos\alpha_n\cos\gamma - \mu\sin\gamma}{\cos\alpha_n\sin\gamma + \mu\cos\gamma}\tan\gamma \approx \frac{\tan\gamma}{\tan(\gamma+\varphi)}$ (worm drives) $\eta_i = \left(\frac{\cos\alpha_n\sin\gamma - \mu\cos\gamma}{\cos\alpha_n\cos\gamma + \mu\sin\gamma}\right)\frac{1}{\tan\gamma} \approx \frac{\tan(\gamma-\varphi)}{\tan\gamma}$ (wheel drives)	α_n normal pressure angle $\gamma = \arctan(m_x z_w/d_w)$ reference cylinder lead angle m_x axial module d_w reference diameter of worm z_w number of threads of worm

- The same type of equations can be established for helical, bevel, epicyclic and hypoid gears, even shifted or corrected.

It is worth mentioning the generic efficiency model of reducers, equations (1) and (2), established in Dohring et al.[13] on the basis of a planar kinematic analogy

$$\eta_d = \frac{1-\mu R}{1+\frac{\mu}{R}} \tag{1}$$

$$\eta_i = \frac{1-\frac{\mu}{R}}{1+\mu R} \tag{2}$$

where R is the dimensionless reduction ratio. This very simple model is equivalent to the simplified expressions for nut–screw efficiencies (when $R = \tan\beta$ or $\mu\tan\beta \ll 1$) and for worm gear efficiencies (when $\cos\alpha_n \approx 1$). Therefore, this model has to be used with care, and only when curvature or three-dimensional (3D) effects remain negligible.

It can be seen that any efficiency model includes the friction factor. Although ball- or roller screw mainly involves rolling contact, efficiency is also calculated as for Acme nut–screws using an 'apparent' sliding friction factor (see Table 2). Unfortunately, calculating a global or equivalent friction factor for a mechanical power transformer is difficult for many reasons:

1. *Influence of lubrication regime*

It is well known[19] that there are typically three regimes of lubrication. This is summarized in Figure 3 which links the friction coefficient to the service number SN

$$SN = \frac{\mu_l V_r}{P} \tag{3}$$

The same shape is sometimes plotted using the Sommerfeld number s instead of SN

$$s = \frac{h}{Ra} \tag{4}$$

Table 2. Effects considered by major friction models for gears.

Author and date	Effect considered						
	Sliding velocity	Rolling velocity	Contact surface roughness	Maximum Hertz pressure at contact	Lubricant viscosity (kinetic or dynamic)	Unit load	Radius of curvature
Misharin (1958)[14]	x	x			x		
Benedict and Kelley (1961)[15]	x	x	x		x	x	
O'Donoghue and Cameron (1966)[16]	x	x	x		x		x
Drozdov and Gavrikov (1968)[17]	x	x	x		x		
IS0/TR 13989 (2000)[18]		x	x	x	x		x

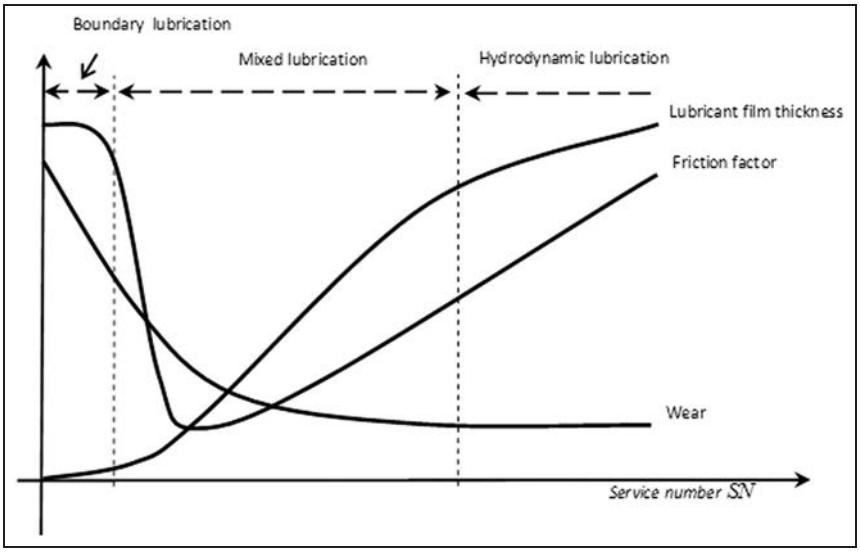

Figure 3. Typical lubrication regimes.

where μ_l is the lubricant dynamic viscosity, V_r is the relative velocity at contact, P is the lubricant pressure at contact, h is the lubricant film thickness and Ra is the surface roughness.

Sliding friction in gears is not negligible and contacts frequently operate in boundary or mixed lubrication regimes, especially for position-controlled actuators where the SN evolves dynamically in the whole domain of lubrication. Unfortunately, these domains still lack generic models.

2. *Sensitivity of lubricant properties to ambient conditions*

The lubricant viscosity that appears as a proportional factor in the hydrodynamic parameter depends exponentially on temperature and pressure, which are not known at the contact location.

3. *Load distribution*

The location of contact points (e.g. in gears) changes periodically with the angular positions of the shafts. In order to enable the global friction factor to be calculated, assumptions must be made concerning load sharing (e.g. among teeth along the contact path line for gears). Since the mid-1950s, this knowledge need has generated numerous proposals for models, as illustrated in Table 2. Unfortunately, each model has its own application range that essentially covers elasto-hydrodynamic lubrication. Therefore, no one model is able to reflect the increase in friction factor in the boundary or mixed lubrication conditions that play a significant role in mechanical power transformers operating around null relative velocity.

An alternative approach[20] is to transit progressively between solid and fluid friction factors (μ_s and μ_l, respectively) according to the relative fluid film thickness ζ

$$\mu = (1 - \zeta)\mu_s + \zeta\mu_l \tag{5}$$

The friction factors are identified as power laws using parametric regressions from experiments conducted versus contact pressure, relative speed and lubricant viscosity.

Bearings. In actuation applications, friction in bearings and joints may be non-negligible, in particular for axial thrust bearings and anti-rotation devices. The component selection process is well documented by manufacturers, including a frictional torque calculation that is mainly addressed using the Lundberg–Palmgren theory[21] where, for non-sealed bearings, friction is seen as the sum of two main physical effects:

1. *The rolling friction torque T_0 comes from hydrodynamic lubrication*

To cope with any quadrant of operation and to facilitate numerical implementation, it is proposed to express it in the condensed form of equation (6) here

$$T_0 = \mathrm{f}_0 d_m^3 \Delta P \left[\max\left(\frac{\mu|\omega_r|}{\Delta P}; 2.10^{-6} \right) \right]^{2/3} \mathrm{sgn}(\omega_r) \qquad (6)$$

with d_m is the bearing mean diameter, μ is the lubricant dynamic viscosity, ω_r is the bearing relative angular velocity and ΔP is the pressure difference between ambient and vapour pressure of lubricant.

The factor f_0, typically between 1 and 9, depends on the type of bearing and the amount of lubricant. When the pressure ratio drops below $2{\cdot}10,^{-6}$ the rolling friction torque becomes independent of speed and is therefore lower bounded to $T_0 = 2 \cdot 10^{-6} \mathrm{f}_0 d_m^3 \Delta P$. That makes it independent of load as well as of speed. Above this pressure ratio, the rolling friction torque is speed dependent. Ambient conditions affect the rolling friction torque through the physical properties of the lubricant (viscosity and vapour pressure).

2. *The sliding friction torque T_1, equation (7), comes from the sliding of rolling elements with respect to facing pieces (e.g. inner and outer rings).*

It also includes the effect of hysteresis in the facing pieces' elastic deformation at loaded contact zones.

$$T_1 = \mathrm{f}_1 F_{e1} d_m \mathrm{sgn}(\omega_r) \qquad (7)$$

The equivalent load F_{e1} for friction calculation is a linear function of axial and radial load components. The function coefficients depend on the type of bearing. In any case, F_{e1} is lower bounded by the radial load component. The factor f_1, equation (8), denotes the sliding friction sensitivity to load

$$\mathrm{f}_1 = k \left(\frac{F_{e0}}{C_0} \right)^n \qquad (8)$$

The sliding friction coefficient k and the exponent n depend on the type of bearing. For a given type, the basic static load rating C_0 depends on the size of the bearing. F_{e0} and F_{e1} are the equivalent loads calculated as linear functions of the radial and axial components of the applied load. The friction parameters depend on the type of bearing and are supplied by manufacturers. Some of them have recently proposed more advanced calculations that combine knowledge models and representation models.[22,23] If relevant, drag and seal friction can be considered as additional sources of frictional losses.

Friction data supplied by manufacturers

There is no uniform approach for providing friction data in catalogues. Component or equipment manufacturers supply different levels of detail using different means. Table 3 illustrates the common practices for nut–screws (ball screw and roller screw), while Table 4 is dedicated to high-performance gear reducers. It is obvious that mechanical losses are incompletely and heterogeneously documented:

1. Efficiency is widely used as the primary means of quantifying frictional losses.
2. In addition to efficiency (see Table 4), breakaway, no-load drive or no-drive back-driving torques are sometimes given.
3. Indirect mechanical efficiency is very rarely addressed.
4. Each manufacturer focuses on the key effects that drive the selection of his components, essentially with respect to mechanical resistance and fatigue. For example, Spinea provides efficiency versus load while HD provides efficiency versus temperature.

Global representation models including load and temperature effects

For sizing, friction modelling can rarely rely exclusively on knowledge models, which may not exist or may have a high degree of uncertainty (at both structure and parameter levels), especially for churning, windage, drag and seal losses. In other cases, for preliminary design at system level, the detailed internal arrangement of the device under study is not known, which makes it impossible to model each source of friction separately. This explains why representation models are so widely used. Three generic means can be employed to establish a representation model of friction:

- Tables are easily implemented in simulation software, where special features often enable variable-order extrapolation and linear/quadratic/spline interpolation. Their main drawback is that they do not provide any explicit information on the nature of friction that could lead to generic knowledge or even facilitate decision making.
- Parametric models can be identified to represent measured data through parameterized mathematical functions of influencing parameters. Polynomial models are simple to generate, but like tables they cannot explicitly display generic effects. Moreover,

Table 3. Example of mechanical losses provided in technical datasheets for high-performance industrial nut–screws.

	NSK ball screws[24]	SKF ball screws[25]	Nook roller screws[26]	Rollvis roller screws[27]	SKF roller screws[28]
Direct efficiency η_d	0.9–0.95	As a function of screw lead, diameter and friction factor $1/(1+\pi\mu d/p)$ $\mu = 0.006$–0.0065 Practical value reduced by 10%	As a function of screw lead, diameter and friction factor (0.038 typically) $1/(1+\mu d/p)$	0.71–0.89	As a function of screw lead, diameter and friction factor $1/(1+\pi\mu d/p)$ $\mu = 0.01$ for $\beta < 7°$ else $\mu = 0.007 * \beta° - 0.04$ Practical value reduced by 10%
Inverse efficiency η_i	0.9–0.95	$2 - 1/\eta_d$ $\mu = 0.01$ for $\beta < 7°$ else $\mu = 0.007 \times \beta° - 0.04$ Practical value reduced by 10%	As a function of screw lead, diameter and friction factor (0.038 typically) $(1 - \mu d/p) = 2 - 1/\eta_d$	0.61–0.85	$2 - 1/\eta_d$ $\mu = 0.01$ for $\beta < 7°$ else $\mu = 0.007 \times \beta° - 0.04$ Practical value reduced by 10%
No-load torque due to preload T_{p0}	$(0.05/\sqrt{\tan\alpha})F_p p/2\pi F_p$ preload axial force	$F_p p(1/0.9\eta_d - 1)/\pi$		$F_p p\mu_e/2\pi$ μ_e equivalent friction coefficient for pre-change (0.1–0.19)	$F_p p(1/0.9\eta_d - 1)/\pi$
Breakaway torque (preloaded)	2–2.5 times the dynamic torque				Twice the dynamic torque

when they are used in dynamic simulation, special attention is needed to avoid unrealistic output values in case of extrapolation outside the validated domain. For this reason, it is particularly attractive to elaborate simple parameterized models of the friction force F_f as a combination of generic effects representing the dependence on load, velocity, quadrant of operation and temperature.

As a general approach, load and temperature effects on frictional losses are introduced, through multiplicative or additive terms, into well-established representation models that already capture the velocity effects. Consequently, in the following sections, the friction models are expressed as a function of translational or rotational velocity (V or ω), transmitted force or torque (F or T) and operating temperature (Θ). These quantities will refer to the drive (subscript D) or load side (subscript L) of the component under study, depending on the causality chosen to express the model. From a practical point of view, the main modelling difficulty lies in obtaining generic models with a reasonable number of parameters.

Dependence of friction on load

Fluid power transformers. In the field of fluid power, a significant amount of friction is generated by high-pressure seals (e.g. in jacks) or motion transformation between a rotating shaft and translating pistons (e.g. in positive displacement pumps and motors). Given the choice made for friction model causalities, it may be found more convenient to use pressure instead of forces (or torques) in the load-dependent friction model as it has a direct influence on normal forces at contact.

1. *Cylinders*

Seals and plain bearings are the only source of friction in cylinders. The action of the chamber pressures P_1 and P_2 on friction is quite linear for a given direction of power, as mentioned in many references, for example, Herrera et al.[33] and Koskinen et al.[34] For sliding conditions, this can be easily introduced into the friction model by using a linear multiplicative term[35] that alters both the Coulomb force F_C and the viscous friction coefficient f through coefficients a_1 and a_2 that apply to chamber pressures P_1 and P_2

$$F_f = (F_C + fV_r)(1 + a_1P_1 + a_2P_2) \tag{9}$$

An alternative solution is proposed in Bonchis et al.[36] as a linear additive term supplementary to the Stribeck and viscous effects. However, no attention is paid to the quadrant of operation

$$F_f = F_S e^{-V_r/V_S} + fV_r + a_1P_1 + a_2P_2 \tag{10}$$

where F_S is the Stribeck force and V_S is the transition velocity of the Stribeck effect.

Table 4. Example of mechanical losses provided in technical datasheets for high-performance industrial nut–screws.

	Load influence	Speed influence	Temperature influence
Wittenstein Alpha, integrated reducers[29]			
No-load running torque	No load	3000 rpm	20 °C
Efficiency	Rated load	Only mentioned	Not addressed
Cyclo-Sumitomo, non-integrated reducer[30]			
No-load running torque	No load	Friction torque versus speed	30 °C
No-load breakaway torque	Single value at null load	Null speed	Not addressed
Efficiency	Rated load	Plot versus speed, from null	20 °C
Compensation factor	Efficiency factor versus load		Not addressed
Spinea, non-integrated reducer[31]			
No-load breakaway torque	Single value at null load	Null speed	20 °C
No-drive back-driving torque	Single value at null load		20 °C
Efficiency	Efficiency versus load	From 500 rpm, 500 rpm steps	45 °C or 60 °C
Harmonic Drive®, non-integrated reducer[32]			
No-load breakaway torque	Single value	Null speed	Not addressed
No-drive back-driving torque	Single value	Not addressed	Not addressed
No-load running torque		From 500 rpm, 500 rpm steps	Plot versus temperature
Efficiency		From 500 rpm, 500 rpm steps	Plot versus temperature

In practice, seal friction depends strongly on the combination of pressure difference and relative velocity and therefore on the direction of power. The pressure distribution on the contact surface of the seal differs when pressure difference and relative velocity are in the same or in opposite directions. This effect has already been reported in Herrera et al.[33] for a single vane rotary actuator (Olaer SS1-A2, 96 cm^3/rev), the friction in which was modelled in a multiplicative way, equation (11)

$$T_f = \left(1 + \frac{T_S}{T_C} e^{-|\omega_r|/\omega_S}\right) [(a_1 + a_2 \mathrm{sgn}(\Delta P \omega_r))\Delta P + T_C]\mathrm{sgn}(\omega_r) \quad (11)$$

with $\Delta P = P_1 - P_2$

Sticking/sliding transitions were implemented using an event trigger approach. This five-parameter model enabled the Stribeck effect, the pressure and the power quadrant–dependent effects to be considered. The measured friction torque was reproduced by the model with a mean relative error of 8.5% for the whole range of four-quadrant operating conditions as illustrated in Figure 4. Note that no viscous effect was identified.

In Kühnlein et al.,[37] the load effect was introduced separately for piston and rod seals, equation (12). For piston seals, it was applied in a multiplicative way to the Coulomb friction and to the Stribeck effect, which were modelled as speed polynomial function. Friction at rod seals explicitly considered the rod diameters and was sensitive neither to preload nor to velocity. The friction model showed a 10% deviation from experiments. Once again, it did not consider the influence of the quadrant of operation.

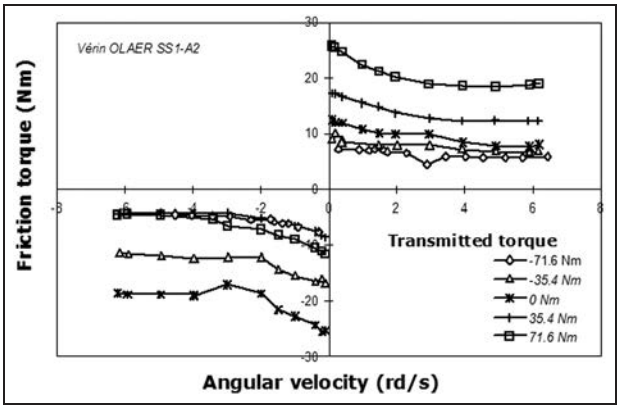

Figure 4. Friction in a single vane rotary hydraulic actuator.

$$F_f = \left[\left(F_C + f|V_r| + a_1\sqrt{|V_r|} + a_2\sqrt[3]{|V_r|}\right)k_p|\Delta P| + \sum_1^2 k_P k_g \Delta P_i\right]\mathrm{sgn}(V_r) \quad (12)$$

Where k_P and k_g introduce sensitivity to pressure and geometry, respectively.

More recently, an additive friction model has been successfully applied[38] for friction modelling in a high-performance, double-rod, symmetrical, hydraulic cylinder (Haenchen HA 80/50). The six-parameter model, equation (13), added together Coulomb, Stribeck, viscous and load-dependent terms. This time, the factor a_2 introduced the influence of the quadrant of operation

$$F_f = \left\lfloor F_C + F_S e^{-|V_r|/V_S} + f|V_r| + |F_L|(a_1 + a_2\mathrm{sgn}(F_L V_r))\right\rfloor \mathrm{sgn}(V_r) \quad (13)$$

where F_L is the force transmitted to load.

The mean error between experimental and simulation results was lower than 10% of the friction force magnitude, which corresponds to a modelling error lower than 0.5% of the cylinder maximum force.

It is important to mention that the non-negligible elastic deformation of seals may lead to a pre-sliding effect (a few 1/10 mm), where relative displacement occurs without sliding. Should this effect need to be simulated, the use of the LuGre friction model[39] with the former equations for sliding conditions will be of interest. Although the intention was not to reproduce pre-sliding, Bo Tran and Yanada[40] used the LuGre model to incorporate load effects, equations (14)–(16)

$$F_f = \sigma_0 z + f\frac{dz}{dt} + \sigma_2\left(V_r + \tau\frac{dV_r}{dt}\right) \tag{14}$$

$$\frac{dz}{dt} = V_r - \frac{\sigma_0 z}{g(V_r, \varsigma)}|V_r| \tag{15}$$

$$g(V_r, \varsigma) = F_C + a_1\left(\frac{F_L}{F_{LR}} - 1\right) + \left[(1-\zeta)F_s - F_C + a_2\left(\frac{F_L}{F_{LR}} - 1\right)\right]e^{-(V_r/V_s)^n} \tag{16}$$

with z the mean deflection of surface asperities, σ_0 the stiffness of elastic bristles, ζ relative fluid film thickness, f the micro-viscous friction coefficient, σ_2 the viscous friction factor, g the function for friction dependency to velocity, F_{LR} the reference value of force to load and σ a shape factor.

First, a first-order lead of time constant τ was added in the friction term of equation (14) in order to account for fluid dynamics and unsteady flow in a gap. Second, the influence of load F_L was introduced into the g function, equation (15), in an additive way. The viscous friction was not affected by the load. As some parameters depended on the relative velocity V_r, the friction model finally involved no less than 20 parameters.

2. *Hydrostatic machines*

Friction in positive displacement hydraulic pumps and motors comes essentially from bearings (sliding or rolling) and dynamic sealing (squeeze fluid films in clearances). In Ivantysyn and Ivantysynova,[41] a generic polynomial representation model is suggested as

$$T_f = \left\lfloor T_C + f|\omega_r| + a_1\omega_r^2 + a_2\Delta P\right\rfloor \mathrm{sgn}(\omega_r) \tag{17}$$

It applies well for operation at permanent velocity. A more generic parameterized model, equation (18), was proposed in Maré[42] for fixed displacement pumps of aerospace electro-hydrostatic actuators. The seven-parameter model was identified using a curve-fitting method from the available measurements, which, unfortunately, were made exclusively under opposite load conditions

$$T_f = \left[T_C + \frac{f}{1 + a_1\Delta P}|\omega_r| + (T_S + a_2\Delta P)e^{-|\omega_r|/\omega_S}\right]\mathrm{sgn}(\omega_r) \tag{18}$$

In this model, the friction dependence on load was introduced as a multiplicative effect on viscous friction and as an additive effect on Stribeck friction. Although the model tended to underestimate friction at low velocities and to overestimate it at high velocities, it was found to be a good compromise between simplicity and accuracy, especially as it applied to a very wide domain of operation, within ±15,000 r/min driving shaft angular velocity and ±220 bar pressure difference at pump use ports.

Mechanical power transmission.

1. *Nut–screws*

With the trend towards more electrical power transmission and control, nut–screws are taking on importance as one of the key mechanical components of linear EMAs. For primary flight controls or even landing gear extension/retraction, roller screw types are being investigated with particular attention as they can withstand high loads without backlash for a 100,000 flight hours, with an extremely low probability of failure. However, increasing the load capacity and removing backlash come at the cost of multiplying the number of contacts between rollers and nut or screw and preloading the nut–screw. This significantly increases friction. For this reason, setting up realistic friction models of nut–screws is a key issue when the intention is to extend the scope of virtual prototyping, thus reducing real testing.

Figure 5 shows the measured efficiency of an inverted roller screw equipped with its bearings (3 mm pitch, 3 kN preload, 50 kN stall force) as a function of the transmitted force at different velocities with opposite and aiding loads. In this mode, the inverse and pseudo-efficiencies clearly point up the presence of the preloading. These data favour the use of the five-parameter friction model, equation (19),[44] which represents the effective friction force with a mean relative error lower than 9.5%. The model introduces a load- and quadrant-dependent Coulomb force in an additive way. Although the quadrant of operation is calculated from the screw to nut angular velocity ω_r and the load force F_L here, different causal choices can be made with no particular difficulty. It is noteworthy that the breakaway force is lower than the Coulomb force, making the 'Stribeck' component negative ($F_S < 0$). This effect has also been reported for other preloaded reducers[43]

$$F_f = \left\lfloor F_C + F_S e^{-|\omega_r|/\omega_S} + |F_L|(a_1 + a_2\mathrm{sgn}(F_L\omega_r))\right\rfloor \mathrm{sgn}(\omega_r) \tag{19}$$

2. *Gearboxes and integrated reducers*

Epicyclic reducers are commonly used in high-performance/long-life embedded applications for their high power density and reduction ratio. Friction in a Cyclo-Sumitomo high-performance cartridge reducer

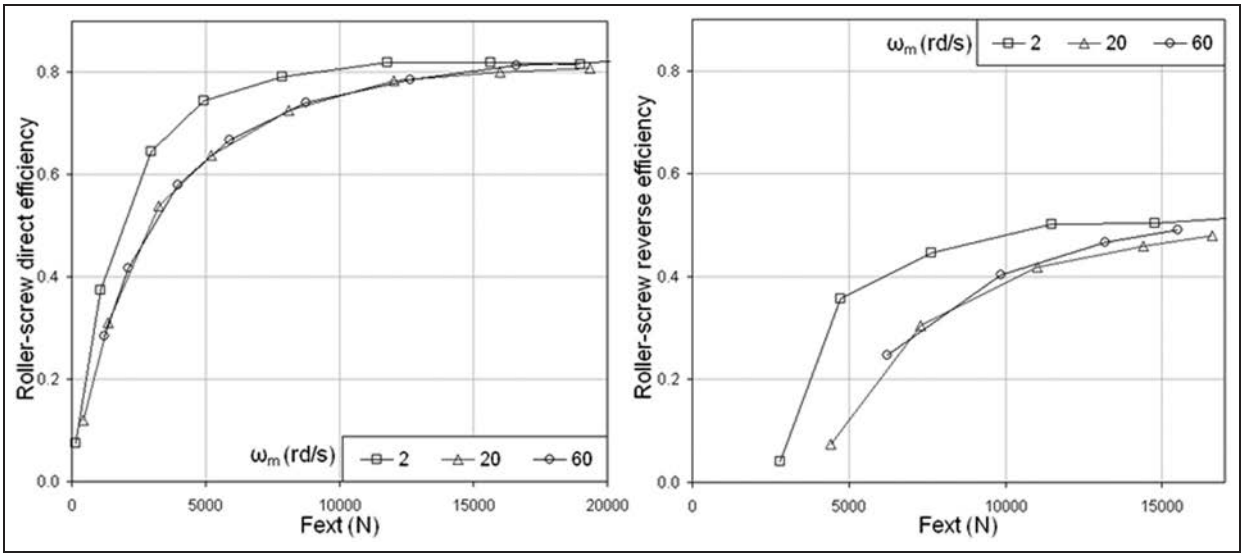

Figure 5. Efficiency of a roller screw equipped with bearings (3 mm pitch, 3 kN preload, 50 kN stall force).

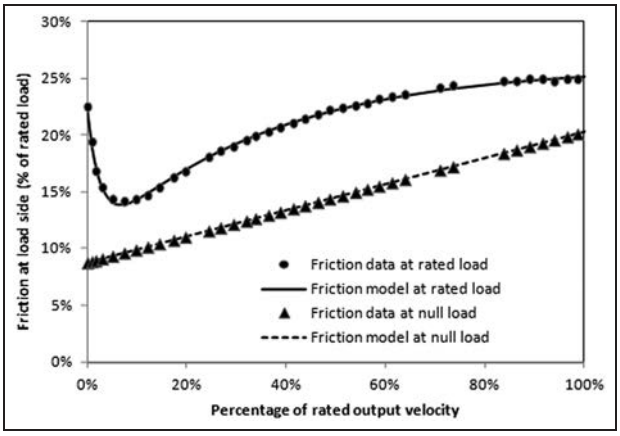

Figure 6. Friction in a Cyclo-Sumitomo epicyclic reducer – model identified from manufacturer's datasheet.

(ratio 59, rated torque 460 N m) has recently been investigated for landing gear steering.[45] The friction model was first identified from manufacturer's data. In addition to tare Coulomb and viscous friction torques (subscripts 0), the best fitting model, equation (20), introduces load-dependent Coulomb, viscous and Stribeck effects (subscripts L) in an additive way to agree with the full-load and no-load data. Velocity ω_D was considered at drive side relative to the housing

$$T_f = \left[T_{C0} + f_0|\omega_D| + \frac{|T_L|}{T_{LR}} \left(T_{CL} + f_L|\omega_D| + T_{SL1}e^{-|\omega_D|/\omega_{S1}} - T_{SL2}e^{-|\omega_D|/\omega_{S2}} \right) \right] \mathrm{sgn}(\omega_D) \tag{20}$$

Once again, it is interesting to note the presence of a negative Stribeck effect. The accuracy of the proposed model can be observed in Figure 6 which displays the modelled versus measured friction for a four-quadrant operation (speeds varying in a 1–5.6 ratio, output torques varying in a 1–28 ratio).

Friction losses were measured on the test actuator where the cartridge reducer was associated with its bearings for integration. A special attention was paid to the breakaway friction torque that was poorly documented in the datasheet. Consequently, the model used for preliminary design, equation (20), was updated as equation (21) which had globally the same additive structure

$$T_f = \left[\left(T_{C0} + f_0|\omega_D| + T_{S0}e^{-|\omega_D|/\omega_{S0}} \right) + \frac{|T_L|}{T_{LR}} \left(T_{CL} + f_L|\omega_d| + T_{SL}e^{-(\omega_D/\omega_{SL})^2} \right) \right] \mathrm{sgn}(\omega_D) \tag{21}$$

The negative Stribeck effect was not observed after integration, a no-load positive Stribeck effect was identified and the shape factor of the load-dependent Stribeck effect was moved from 1 to 2. Finally, the nine-parameter model introduced a mean relative modelling error lower than 2%. Most of the modelling errors remained within the ±20% range, as shown in Figure 7.

In a more global approach, the dependence of friction on load was represented by a five-parameter model, equation (22), that was identified dynamically for robot joints.[46] Load effects were once again introduced in an additive way in the speed-independent and Stribeck terms

$$F_f = \left[a_1|T_L| + a_2 + (a_3|T_L| + a_4)e^{-|V_r|/V_S} \right] \mathrm{sgn}(\omega_D) \tag{22}$$

In a general approach, parameters a_1–a_4 may take different values according to the direction of power.

3. *Harmonic Drive reducers*

The influence of load on friction in HD reducers has been identified in Hospital[5] for lubrication with an aerospace grease at 20 °C. An additive model was found to be adequate, which added load-proportional Coulomb, viscous and Stribeck friction, equation (23)

$$T_f = \left[\left(T_{C0} + f_0|\omega_D| + T_{S0}e^{-|\omega_D|/\omega_{S0}}\right) + \frac{|T_L|}{T_{LR}}\left(T_{CL} + f_L|\omega_D| + T_{SL}e^{-|\omega_D|/\omega_{SL}}\right)\right]\mathrm{sgn}(\omega_D) \quad (23)$$

4. *Worm gears*

In the same application of EMA landing gear steering,[45] a worm gear was used as the final reducer. The friction losses were first calculated as mentioned in Table 1 by introducing the Stribeck effect in the friction coefficient

$$\mu = \mu_\infty + (\mu_S - \mu_\infty)e^{-(|V_r|/V_S)^n} \quad (24)$$

where μ_s is the static (null speed) friction coefficient and μ_∞ the limit (infinite speed) friction coefficient.

The four parameters of the friction model were first identified from suppliers' data with generic grease properties. The model was updated after testing, in particular to include bearing friction and aerospace grease properties. Although the friction coefficients were only increased by 9%, the reference velocity was multiplied by 10 and the shape factor increased by 40. A constant Coulomb friction was added to reflect friction of the seals. The 95% confidence interval of the friction model is illustrated in Figure 8. As measurements were taken using a mounting with two worm gears face-to-face, the friction torques given are the sum of direct and indirect quadrant effects. As for the Cyclo reducer, the effect of integration is important. For the worm gear, integration increases frictional losses by 50% relative to pure gear mesh considerations, in particular due to the high combined loads (axial and radial) applied to bearings in worm gear reducers.

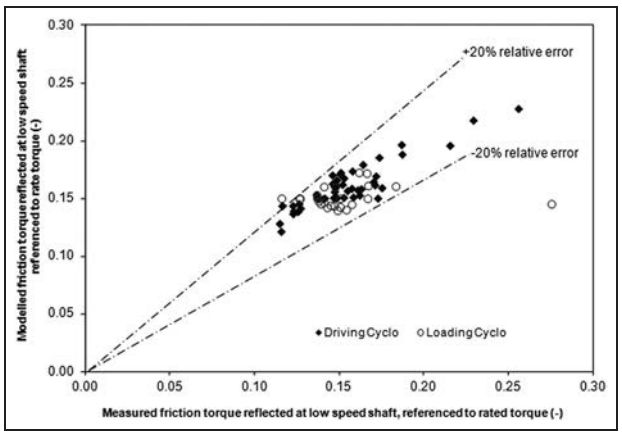

Figure 7. Friction in a Cyclo-Sumitomo epicyclical reduced – identification from actuator testing.

Dependence of friction on temperature

In embedded actuation applications, for example, aerospace, actuators must meet the performance requirement over a wide range of temperature (e.g. −40 °C to + 70 °C). Unfortunately, frictional losses tend to increase drastically at low temperatures. The major effect comes from the sensitivity of friction factor to temperature. Another effect may be induced by

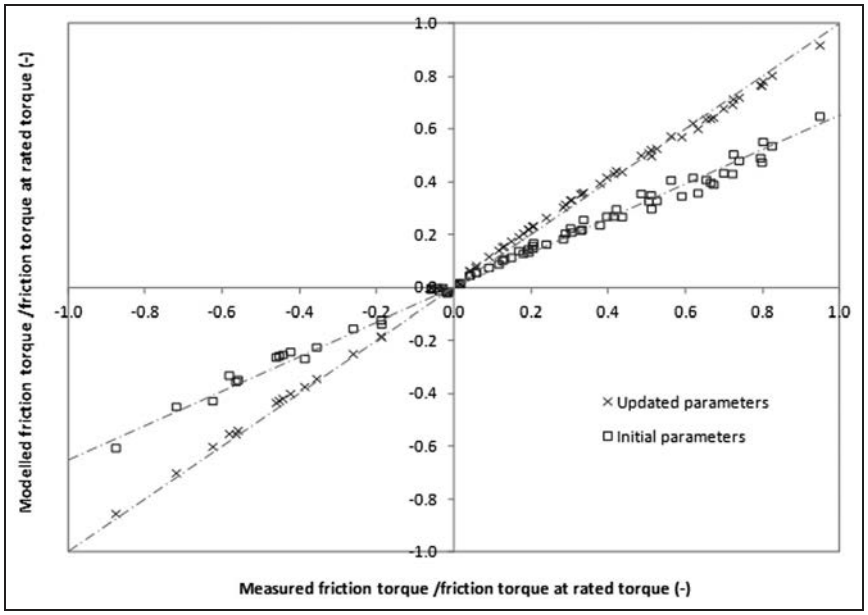

Figure 8. Modelled friction torque versus measured friction torque for a worm gear (with and without integration effects).

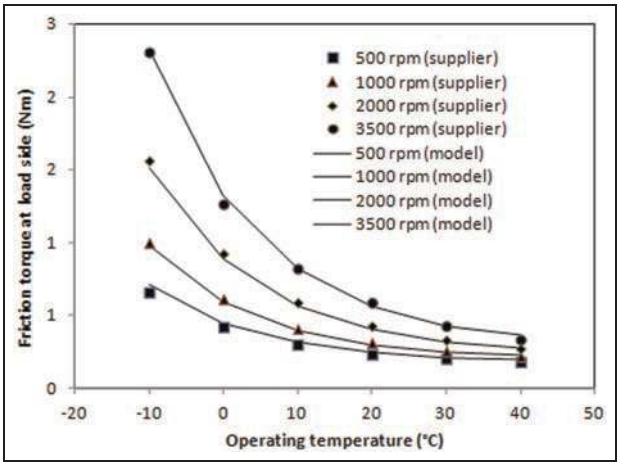

Figure 9. Influence of temperature on friction torque calculated for Harmonic Drive® efficiency data (size 14, ratio 100).

dilatation of solids that affects the amount of preloading. A good illustration of the influence of temperature is given by the efficiency data provided by HD reducers.[32] Figure 9 shows the friction torque calculated from efficiency data as a function of temperature for different velocities (HD reducer size 14, ratio 100). For such a reducer, the friction torque varies by a factor of 1.8 (at 500 r/min) to 3.5 (at 3500 r/min) when the temperature changes from −10 °C to + 40 °C.

Knowledge models of friction sensitivity to temperature are not well established, even at microscopic level.[47] At component or equipment levels, this sensitivity can be introduced by representation models in different ways. A first idea would be to consider the influence of temperature on lubricant viscosity, which finally impacts the friction factor. In Gruebler and Hora,[48] the dynamic friction during metal forming is simulated using a temperature multiplicative model of the friction coefficient

$$\mu(\Theta) = \mu_0(V_r)\left(1 - a_1 V_r e^{a_2/(\Theta + a_3)}\right) \tag{25}$$

where a_1, a_2 and a_3 are constant parameters and Θ is the temperature. The model is validated for a temperature range of 23 °C–100 °C for relative velocities varying from 7 to 160 mm/s.

The temperature effect was introduced in Li et al.[49] for an unloaded micro-motion actuator by modifying the standard LuGre friction model. Additive and multiplicative models were compared, each one adding six parameters. In the multiplicative form, the stiffness (σ_0) and damping (f, σ_2) parameters were replaced by linear or exponential functions of temperature. In the additive form, the temperature-dependent friction was introduced as a dual-slope linear function of temperature. The second approach was found to be simulated faster with higher accuracy. However, the proposed model was validated for a very narrow temperature range of 30 °C–41.5 °C. The same idea of modifying the generalized friction model was proposed in Bittencourt et al.[50] for robot joints. The friction model was decomposed into three additive terms, equation (26)

$$\begin{aligned} T_f = &\left\{ T_{C0} + \frac{T_{CL}}{T_{LR}}|T_D| + T_{SL}|T_D| e^{-(|\omega_r|/\omega_{SL})^{1.3}} \right\} \\ &+ \left\{ T_{S0} + T_{S\Theta}\Theta \right\} e^{-[|\omega_r|/(\omega_{S\Theta} + a_1\Theta)]^{1.3}} \\ &+ \left\{ \left(f + a_2 e^{-\Theta/\Theta_R} \right) \omega_r \right\} \end{aligned} \tag{26}$$

where Θ_R is the reference value of temperature.

The first two terms modelled the velocity-weakening friction with its dependence on load and temperature. The last term modelled the velocity-strengthening regime with dependence on temperature only. The 11 parameters of the model were identified in the range 38 °C–81 °C, up to 300 rad/s. The temperature range addressed in these models was still narrow in comparison with that of embedded systems, especially at low temperatures.

For preloaded gears, like HD reducers, the temperature effect can be introduced in a multiplicative way here, acting on all friction parameters. A five-parameter friction model, equation (27), suits the catalogue data of HD reducers well, as shown in Figure 9. For example, for a CFG model size 14 ratio 100, the relative modelling error remains lower than 8% with a mean value lower than 0.6%

$$\begin{aligned} T_f = &\left[T_C \left(a_1 + a_2{}^{-\Theta/\Theta_R} \right) \right. \\ &\left. + f\left(a_3 + a_4{}^{-\Theta/\Theta_R} \right) |\omega_D| \right] \mathrm{sgn}(\omega_D) \end{aligned} \tag{27}$$

It can be observed that the proposed model does not involve any Stribeck effect in addition to Coulomb and viscous ones as the catalogue data concern only velocities greater than 14% of the rated value. Consequently, the present generic friction model is not validated in the region of null speed where position actuators operate most of the time. In order to extend the model application range to stuck conditions, specific measurements were taken in Hospital[5] to investigate the influence of velocity, load and temperature. Tests were run for the whole range of loads and velocities (opposite and aiding loads) on a CPU-32-50-M reducer (ratio 50, size 32, aerospace grease) supplied by HD. The temperature was varied from −20 °C to 60 °C. This was essentially intended to capture the low and high extreme conditions for speed, load and temperature. The nine-parameter model, equation (28), was successfully used by varying each friction model parameter as an exponential function of temperature, adding 10 extra parameters

$$\begin{aligned} T_f = &\left[T_{C0} + f|\omega_D| + T_{S0} e^{-|\omega_D|/\omega_{S0}} - T_{S1} e^{-|\omega_D|/\omega_{S1}} \right. \\ &\left. + \frac{|T_L|}{T_{LR}} \left(T_{CL} + T_{SL} e^{-|\omega_D|/\omega_{SL}} \right) \right] \mathrm{sgn}(\omega_D) \end{aligned} \tag{28}$$

A generic frame for modelling friction at system level

When the intention is to generate real added value for virtual prototyping, considering modelling alone is not sufficient. Developing a library of component models does not eliminate the need to offer major features such as reusability, genericity and capitalization. For this reason, it is worthwhile to address proposals for model parameterization, implementation, causality and structure.

Parameterization of friction models

At the modelling stage, the major friction effects that fix the overall performance of the system under design have to be reproduced in a realistic way, in relevance with the design activities concerned. The velocity, load and temperature effects are time varying, non-linear and coupled. In addition, special attention has to be paid to friction forces at null speed or in aiding load conditions, which may impact performance very significantly.

As mentioned in the previous sections, different approaches can be used for modelling friction in mechanical engineering:

1. *Mechanical efficiency*

This essentially supports sizing activities of power transformation devices like reducers or nut–screws. By its structure, efficiency implicitly reproduces the dependence of friction on load. It is expressed from the drive and load forces depending on the mode of operation. The direct efficiency η_d refers to the functional mode of operation where power flows from drive to load (opposite load). The indirect efficiency η_i is used when the load aids motion, the power flowing backwards from the load to the drive (aiding load). Pseudo-efficiency η_p links the drive side and load side loads under aiding load when the power transformation is non-reversible (power also has to be input at the drive side under aiding load conditions). For most of the contact losses in power transformation devices (e.g. nut–screw), efficiency can be expressed analytically, as illustrated in Table 1, from geometrical data and the effective friction factor μ. This helps to formally identify the influence of design choices on efficiency. Unfortunately, using a single value of efficiency provides the designer with a weak indication of frictional losses for many reasons:

- For a given lubricant, efficiency depends on speed, load and temperature, including dependency on the quadrant of operation (the direction of power).
- Efficiency is rarely known (from equations or from manufacturers' data) in aiding load conditions or for intermediate power in opposite load conditions.
- Using efficiency does not enable the designer to calculate frictional forces when the input or output powers are null: at null speed, at null input torque (no-drive back-driving torque or force) or at null output torque or force (no-load driving torque or force).

Therefore, using only efficiency for friction modelling may lead to serious errors. On the one hand, for power sizing of more electrical drives that require the mean values of the power variables to be calculated from the mission profile, failure to consider the no-load driving torque often leads to drastic over- or undersizing depending on the load characteristic and backdrivability. On the other hand, for control performance, static accuracy and stability can be highly dependent on breakaway friction.

2. *Equivalent friction factor*

The concept of using the friction factor comes from sizing with respect to wear. It applies well to special types of mechanical power transformers (e.g. worm gears or nut–screws) where friction loss can be expressed explicitly as a function of friction factor by using mechanical force balance and contact geometry. Its main advantage is that the amount of friction loss can be analytically linked to sizing variables like diameter and pitch. However, this approach cannot be generalized to all kinds of component. Moreover, it moves the problem of friction dependency on velocity, load and temperature to their effects on the friction coefficient.

3. *Amount of friction force*

Friction force is a direct indicator of force loss. It applies well when other means of characterization cannot be used (no mechanical model or no power transmitted). Speed-dependent friction has been commonly used for decades to deal with control design. The perfect viscous friction model is extremely convenient for dynamic analysis and control design, which generally starts with a linear model. As a logical extension, many model improvements have been proposed to better represent the non-linear dependency at low velocities (Stribeck effect) or high velocities (windage effect). It is interesting to note that although they are well established and documented, speed-dependent friction models provide a very unrealistic representation of friction in power transformation devices because relative velocity is only one of the key influencing factors.

Model implementation

In the simulation phase, implementation of the friction model must avoid abrupt discontinuities that generally induce numerical instabilities, especially for transitions between sticking and sliding. In sliding conditions, friction is a sign function of relative velocity and its

magnitude depends on several factors (velocity, load, temperature, etc.). In the basic Coulomb friction theory, the friction force F_f is linked to the normal force F_N at contact through the friction factor μ

$$F_f = \mu F_N \mathrm{sgn}(V_r) \tag{29}$$

In stuck conditions, when the relative velocity is null, the friction force F_f opposes other forces to avoid relative motion up to breakaway. In the basic Coulomb model, this condition is given by

$$|F_f| < (\mu F_N \cdot (F_N > 0)) \tag{30}$$

In practice, the transition between stuck and sliding modes can be handled in various ways:

1. *Linearizing the sign function by a hyperbolic tangent*

In sliding conditions, the direction of the friction force depends on the sign of the sliding velocity. Replacing the *sign* function by a hyperbolic tangent function is a straightforward and simple way to make the friction model continuous with respect to relative speed V_r. Thus, it generally avoids having to handle numerical instability in the vicinity of null speed

$$\mathrm{sgn}(V_r) \approx \tanh\left(\frac{V_r}{V_R}\right) \tag{31}$$

where V_R is the reference velocity and is typically set to 1/10,000 of the rated value.

The main drawback of the model is its inability to reproduce true stiction when friction balances other forces at exactly null relative speed. However, when V_R is properly set, the force balance is satisfied for a very low velocity that can be considered as null for response analysis. Note that, in very special conditions or with some non-causal solvers, the *tanh* model may introduce instability.

2. *Forcing velocity to null when sufficiently low*

The Karnopp model[51] forces velocity to null when its magnitude becomes lower than a threshold value. The friction model must be embedded in a mass or inertia model and cannot be dissociated from it, even if it is not intended to model any inertial effect. Karnopp friction models do not work when multiple friction locations are considered.

3. *Using a state machine to switch between modes*

In this case, an event-triggered machine is implemented to switch between friction models when mode changes (sticking or sliding), for example, *LossyGear* model of the Modelica Standard Library, based on Otter et al.[52]

4. *Modelling pre-sliding effects (Reset, Dahl, LuGre)*

Modelling the pre-sliding regime, with contact compliance in stuck conditions, changes the model from two switched algebraic equations into a single continuous differential equation. As explained in Karam and Maré,[4] Reset integrator, Dahl and LuGre models are well established and available as standard friction models in simulation software, for example, LMS-AMESim. Although considering pre-sliding is rarely necessary at system-level modelling and simulation, this option is often used as a means of fixing the numerical issue around the null relative velocity. Unfortunately, these types of models involve additional, and unknown, parameters and increase the simulation time.

Friction and inverse simulation

Being widely available in recent non-causal modelling languages, for example, Modelica, inverse simulation provides the designer with efficient means of power architecting and sizing: the power demand is given at load level and can be propagated backwards by inverse simulation to the power sources. In this procedure, modelling friction faces a very specific issue: a (rigid) friction model is not physically invertible at null speed. For inverse simulation, all that is known is that friction force opposes other forces. Consequently, there is an infinity of combinations of driving forces and friction forces for a given force to load provided by the mission profile. In practice, the effective drive force in stuck conditions depends on the non-linearities of upstream power devices (e.g. hysteresis or quantization) and control laws. For inverse simulation, under-determination is magnified in the presence of multiple friction sources acting on the same rigid body. Well-established rigid friction models do not solve this issue. For example, at null velocity, the *tanh* model outputs null friction, while the *LossyGear* model considers implicitly that the load (flange b) is aiding. Three options can be suggested to manage this situation:

1. The simplest one adds a hysteresis function that holds the friction torque to its latest value when stopping occurs. However, special care must be taken not to generate mechanical power by the modified friction model during mode transition.
2. In another approach, a real parameter in the range $[-1; 1]$ is introduced in order to force the calculation of the drive torque or force.[53] For -1, the drive torque is about to start motion against the load, while for $+1$ the drive torque tends to start motion with the load. The parameter can be set to extreme values or varied randomly to assess the sensitivity of sizing to friction forces.
3. The third solution is to introduce pre-sliding effects as mentioned in the former section, at the expense of increased complexity, number of parameters and simulation load.

Structure of a generic friction model

The generic scheme of Figure 10 will be used in the following developments related to friction modelling. The

friction effect is isolated from other effects in order to facilitate the discussion and the modelling. Although the model is given for linear motion, it can be adapted without restriction to the rotational case, replacing forces F by torques T and linear velocity V by angular velocity ω. For power transformation devices, a perfect (no loss) reducer has to be added upstream or downstream of the friction model, with the adequate transmission ratio. The frictional loss is considered as a single lumped effect. It may represent friction in integrated equipment items or a combination of lumped effects induced by components. The friction loss model can be reduced either at the drive side or at the load side.

The friction force F_f developed at the interface between the base and the mobile is influenced by the normal contact force F_N that balances the external normal force F_{NE}. The forces F_D and F_L are the force applied from the motor side and the force transmitted to the load side, respectively. The absolute base position and velocity are noted X_b and V_b, respectively. The relative motion X_r and velocity V_r are defined from the base and mobile positions (X_b, X_M) and velocities (V_b, V_M) as

$$X_r = X_M - X_b \tag{32}$$

$$V_r = V_M - V_b \tag{33}$$

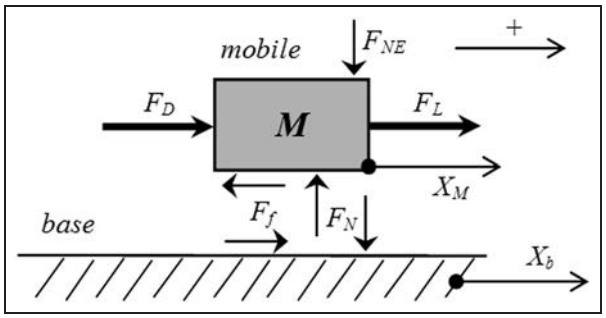

Figure 10. Schemes and notations for friction modelling.

Newton's second law applied to the mobile of mass M, in projection on the translational axis, gives the force balance as

$$F_D - F_L - F_f = M\frac{dV_M}{dt} \tag{34}$$

It can be observed that

1. The sign convention used for friction force corresponds to a resistive view.
2. Although friction depends on the relative velocity V_r, the force balance involves the absolute, not the relative, acceleration of the mobile.
3. The inertial force, the right-hand term of equation (31), is not part of the friction model.

As already mentioned, the friction force typically depends on relative velocity, drive or load force, temperature and time.

A generic frame for modelling friction at system level

A generic frame is proposed as a Bond-graph (Figure 11) for structuring and implementing the equations of a friction model. It does not impose any specific constraint to the management of the sticking/sliding transition, to the implementation of velocity, load and temperature effects (parameterized function, look-up tables, etc.) or to causality (works with causal as well as non-causal simulation software). The friction model does not require inertia to be considered. If necessary, inertia can be introduced at either the drive or the load side.

The equation defining the friction force versus velocity, load and temperature (e.g. equation (28) for rotational devices) is used as the constitutive equation of a modulated resistor-field (MRS). The friction dependence on velocity is considered by definition of the Bond-graph R element that links the friction force F_f to the relative velocity V_r. Friction is made dependent on

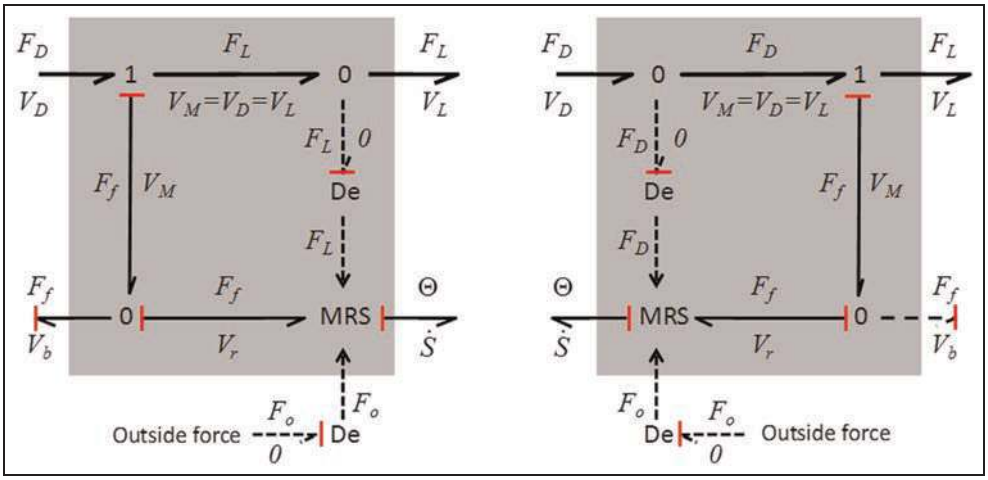

Figure 11. Generic frame for friction modelling.

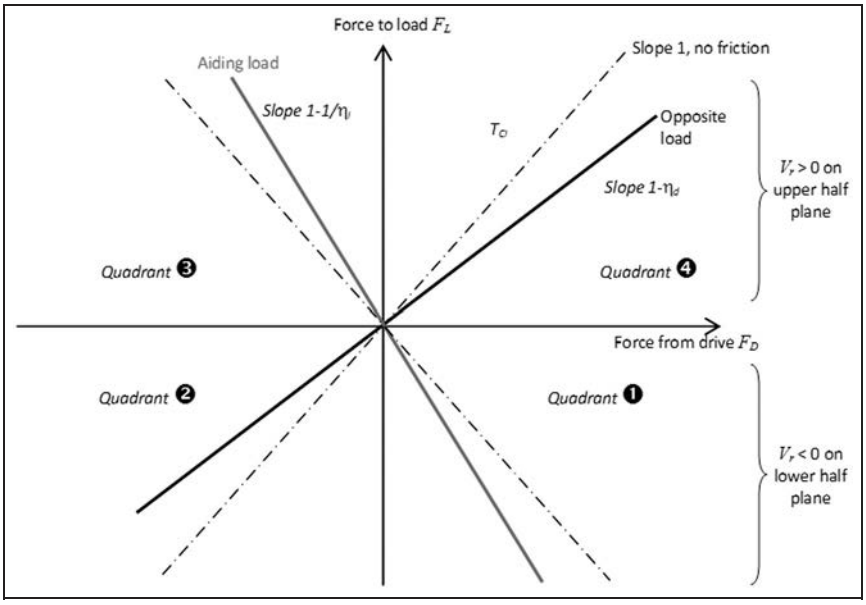

Figure 12. Mapping the load and drive force according to quadrant of operation (constant efficiencies assumed).

load by the modulating input M of the MRS element. Load effect can be introduced in two ways:

Internally. This approach is well suited to the modelling of friction in power transmission elements, for example, reducers, where friction can be linked to the transmitted force F_L or the received force F_D. The modulating signal comes for a detector element (DE) that plays the role of an ideal force sensor. Force is sensed from the power domain without parasitic motion or velocity loss and is propagated to the signal domain.

Externally. This applies well to bearings and joints. In this case, friction is influenced by an outside load F_o, for example, the normal external force F_N of Figure 10 that is not directly in the power path of the friction model.

Friction sensitivity to temperature is implemented, thanks to the S effect of the MRS element, which denotes the irreversible transformation of friction energy into heat. It is advantageous to use a thermal bond to link the mechanical and the thermal domains through pseudo-thermal power variables. On the one hand, the heat generated by friction (entropy flux dS/dt) is made available for system-level thermal modelling. One the other hand, the temperature Θ can be used to vary the friction force, for example, with parametric models as given in section 'Dependence of friction on temperature'.

The '0' junction associated with the DE enables force to be sensed. The 0 junction connected to the MRS element generates the speed relative to the base motion, equation (33) while it propagates the friction force on the load or drive port and on the base port according to the action/reaction principle. The '1' junction subtracts the friction force to the drive force to make the force to load. As the inertial effect is not part of the friction model, this junction implements equation (34). It also imposes the velocities of the points of application of these forces to be identical.

Causalities

Causality marks have been added in Figure 11 when there is no alternate choice in practice:

- The DE detectors shall get force and impose null loss of velocity.
- The MRS element shall calculate the friction force F_f versus the relative velocity V_r to avoid indetermination in case of non-monotonic dependence of force to speed (e.g. Stribeck effect).
- The MRS element shall output the heat power dS/dt generated by friction loss in order to avoid indetermination and shall get temperature Θ to impact the friction force.
- As already mentioned, the 0 junction shall propagate the friction force according to the action/reaction principle.

Except these constraints, causalities are free at load and drive ports, as far as they meet the internal causal rules of the friction model:

- For well-established direct simulation, either the pair (F_D, V_L) or the pair (F_L, V_D) can be imposed.
- When inverse simulation is permitted, either the pair (F_D, V_D) or the pair (F_L, V_L) can be imposed.

Determination of the power quadrant

As the friction force generally depends on the quadrant of operation, the friction model requires knowing the sign of power. This can be obtained by taking force

either at the drive or at the load side. In Figure 11 (left), the power quadrant is calculated from the load side (opposite or aiding load), while it is calculated from the drive side (drive acts on the friction model as a motor or as a generator) in Figure 11 (right). Special attention must be paid to the importance of this choice that may significantly impact the calculated friction force when the drive or load force is in the same range of magnitude as the friction force. Indeed, in this particular situation, the power quadrant may be different, but with same velocity, at drive and load sides.

Finally, the proposed frame for the friction model makes it fully balanced, at mechanical level (the base has to withstand the friction force) as well as at power level (the heat balance is verified at any time for the model). It is interesting to notice that these two properties are rarely verified in most of the friction models implemented in commercial simulation libraries. However, modelling progressivity may take benefit of optionally enabled base and thermal ports. The friction model is autonomous and can be inserted in any power path without requiring inertia to be considered and can be run with any possible causality.

Modelling friction losses from mechanical efficiency

It has already been mentioned that using mechanical efficiency to model friction is attractive because of its very common use in design. Two options arise: either to translate efficiency data into a friction force model explicitly or to develop a friction model directly from efficiency data without explicit calculation of the associated friction force.

Obtaining friction force from efficiency data

Depending on the type of efficiency data, the friction force can be obtained either formally or by identification.

Calculation of friction force from efficiency. According to the notation of Figure 10, direct efficiency η_d is defined when the power flows from the functional drive to the load side

$$\eta_d = \left|\frac{F_L}{F_D}\right| = \left|\frac{F_L}{F_L + F_f}\right| = \left|\frac{F_D - F_f}{F_D}\right| \tag{35}$$

Indirect efficiency η_i is defined when the load is back-driving (adding load) making the power flow opposite to the functional direction

$$\eta_i = \left|\frac{F_D}{F_L}\right| = \left|\frac{F_D}{F_D + F_f}\right| = \left|\frac{F_L - F_f}{F_L}\right| \tag{36}$$

At this step, some of the following important remarks can be made:

1. When the load tends to back-drive a non-reversible component, it is also necessary to input force from the drive side to generate motion. In this case, a pseudo-efficiency η_p can be defined as the ratio of load to drive force magnitudes.
2. The absolute function in equations (35) and (36) is mandatory (although generally omitted) for application to any power quadrant, as both driving and load forces can be either negative or positive.
3. It should be recalled that modelling frictional losses with efficiency leads to under-determination of friction forces when the transmitted power is null. This important drawback will be addressed later.

Inverting equations (35) and (36) enables the friction force to be linked to efficiency and load/drive forces. By paying special attention to the quadrant of operation, it is possible to obtain the following equations, which apply whatever the sign of the load force

$$\text{For opposite load} \quad F_f = F_L\left(\frac{1}{\eta_d - 1}\right) \quad \text{or} \quad F_f = F_D(1 - \eta_d) \tag{37}$$

$$\text{For aiding load} \quad F_f = F_L(\eta_i - 1) \quad \text{or} \quad F_f = F_D\left(1 - \frac{1}{\eta_i}\right) \tag{38}$$

A simple mechanical loss model can therefore be developed using efficiency data and switching between direct and indirect modes according to the sign of the power flowing from drive to load (Figure 12). The direction of power is calculated either from the drive side force or from the load side force depending on the causality chosen for the model. Although the following developments consider the second option, there is generally no special difficulty in using the first one for model implementation.

As highlighted in Figure 12, using efficiency for modelling friction losses makes the friction model continuous versus load (or drive) force for a given sign of velocity. Conversely, it is strongly discontinuous when the sign of the velocity changes, switching between the upper and lower half planes of the figure. Without paying attention to the change in quadrant, a compact model can be obtained by introducing logical conditions in the equation of the friction force

$$F_f = \left[\left(\frac{\eta_d}{\eta_d - 1}\right) \cdot (F_L V_r > 0) + (\eta_i - 1)(F_L V_r < 0)\right] F_L \tag{39}$$

or

$$F_f = \left[(1 - \eta_d) \cdot (F_D V_r > 0) + \left(1 - \frac{1}{\eta_i}\right) \cdot (F_D V_r < 0)\right] F_D \tag{40}$$

If the intention is to make the model continuous by replacing the sign functions by hyperbolic tangent

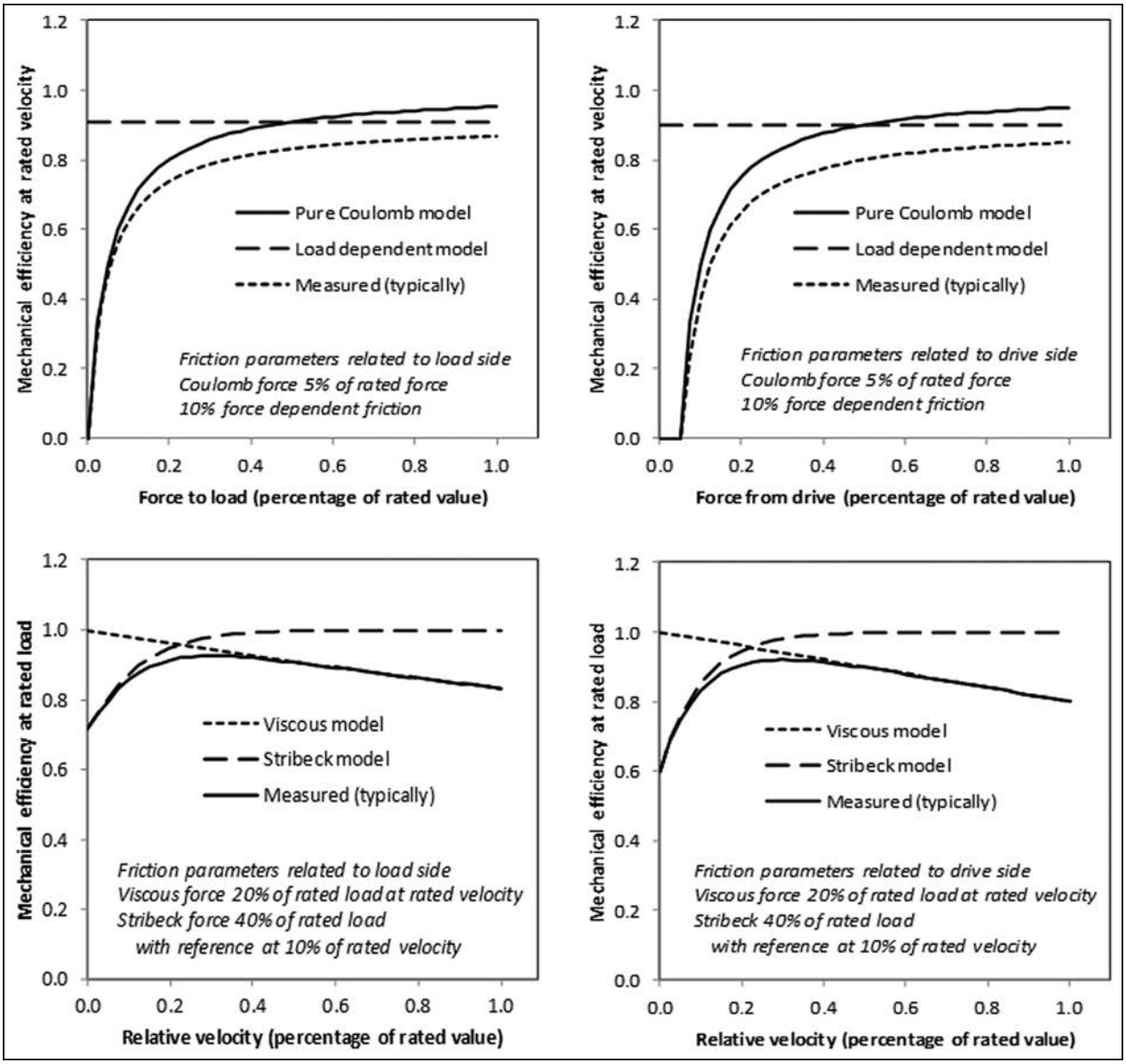

Figure 13. Friction model structure from efficiency plots. Load (top) and velocity (bottom) effects separated.

functions, a reference value has to be defined, not only for velocity but also for power. The model therefore involves two hyperbolic tangent functions that may require excessively small integration steps to accurately detect the change in quadrant of operation. Thus, defining a reference power that is consistent with the reference velocity becomes a tricky task. In addition, the friction model must transit between quadrants in the same manner whatever the causality chosen for the force input. This is hard to achieve. For all these reasons, it is proposed to remove these drawbacks by noting that

$$F_D \mathrm{sgn}(F_D V_r) = |F_D| \mathrm{sgn}(V_r) \quad \text{or} \quad F_L \mathrm{sgn}(F_L V_r) = |F_L| \mathrm{sgn}(V_r) \tag{41}$$

Consequently, the sign of velocity can be used instead of the sign of power, making the model implementation simpler and its computation faster around null drive or load force.

Identification of friction model from efficiency. As illustrated in Tables 3 and 4, it is common practice to quantify frictional losses in mechanical power transformers with efficiency plots versus relative speed and driving (or load) force, plain lines in Figure 13. As developed below, a detailed understanding of the shapes of the plots is of great help when aiming to identify the structure of a friction model having minimal complexity.

As illustrated in Table 5, key information is provided to accelerate the identification process of the friction model structure. It suggests reproducing load or velocity effects separately by an additive combination of the basic friction effect. For special designs where components run at very high velocities, it may be necessary to add a quadratic dependency of friction on velocity to

Table 5. Basic friction effects and their influence on efficiency.

Friction model	Direct efficiency (positive velocity)	Friction model parameter
Friction dependency on load		
$F_f = F_C \mathrm{sgn}(V_r)$	$\eta_d = \frac{1}{1 + F_C/F_L}$	$F_C = \left(\frac{1}{\eta_{dr}} - 1\right) F_{LR}$ at rated operation point
$F_f = aF_L$	$\eta_d = \frac{1}{1 + a}$	$a = \frac{1}{\eta_d} - 1$
Friction dependency on velocity		
$F_f = fV_r$	$\eta_d = \frac{1}{1 + fV_r/F_L}$	$f = \left(\frac{1}{\eta_{dR}} - 1\right) \frac{F_{LR}}{V_{rR}}$ at rated operation point
$F_f = F_s e^{-\lvert V_r\rvert/V_S}$	$\eta_d = \frac{1}{1 + \frac{F_S e^{-\lvert V_r\rvert/V_S}}{F_L}}$	

obtain a better model at the expense of one additional parameter.

As suppliers practically never provide friction data for aiding load conditions, it is useful to find a first estimate of inverse efficiency by assuming the friction force to have the same magnitude whatever the direction of power. Under this condition, combining equations (35) and (36) yields

$$\eta_i = 2 - \frac{1}{\eta_d} \tag{42}$$

which gives positive values only if $\eta_d > 0.5$ (reversible transmission).

Although this relation applies very well to nut–screw friction models as long as $\mu \tan(\beta) \ll 1$, which is satisfied most of the time, it may introduce significant errors. In particular, it tends to overestimate friction in aiding load conditions for HD reducers.[5]

Finally, combining pure Coulomb friction with load-proportional (or dependent), viscous and Stribeck friction enables the measured efficiencies to be reproduced with a minimal parametric friction model: the model involves only five parameters that are easily identified. An additive combination generates the overall friction force by summing load- and velocity-dependent friction forces. In a multiplicative combination, the Coulomb and velocity-dependent friction members are multiplied by the amount of load. The latter approach is more representative of the physical effects where normal forces at contact directly influence the thickness of the lubricant layer and/or the amount of solid contacts between the moving bodies. In practice, the two approaches are mixed, as illustrated in section 'Global representation models including load and temperature effects'.

Direct use of efficiency in friction model

Efficiency can also be used explicitly in a friction model. However, because of its inability to deal with friction at breakaway, it is mandatory to add a friction force to the efficiency model. This can be seen as the series combination of friction loss at contact points in positive power transmission (modelled by efficiency, for example, from Table 1) and of other load-independent friction forces due to seals, bearings and churning (modelled by additional friction force). This approach is typically implemented in the *LossyGear* model for gear reducers according to Pelchen et al.,[54] considering in series the following:

- A speed- and quadrant-dependent friction as tare loss (that is not influenced by load-independent friction torque), using a Coulomb model with different values for opposite and aiding load operations.
- A load-dependent friction, modelled using direct and indirect efficiency tables according to speed and quadrant.
- Perfect power transformation (no power loss).

For both aiding and opposite loads, the model parameters are assumed not to be sensitive to the sign of the velocity. Moreover, the model parameters do not correspond to the common catalogue data. This still requires extra data handling from the designer.

Conclusion

The review and synthesis of common friction simulation practices published in Karam and Maré[4] pointed out the weakness of system-level simulation models regarding the influence of load and temperature effects on friction. On this basis, this work was intended to address these effects in a practical way for scientists and engineers involved in system-level activities, especially for embedded power transmission and motion control. The first action established a detailed review and synthesized the state of the art and usual practice, with detailed consideration of models for sizing, data supplied by manufacturers and representation models for virtual prototyping. It was shown that models and data are globally not consistent and are not sufficiently complete to support system-level model-based design. Numerous validated representation models reflecting load and temperature effects were introduced and discussed. Two approaches were investigated. In the first one, friction losses were modelled with explicit reference to friction forces by a combination of generic effects (Coulomb, viscous, Stribeck), completed by

introduction of load and temperature effects as additive or multiplicative terms. The second one explicitly involved the mechanical efficiency, which naturally introduced the influence of load. It was shown that using efficiency raised various issues, especially for sticking. In order to facilitate the development of realistic system-level friction models, a generic friction model frame was proposed that is compatible with both approaches and enables thermal balance analysis to be performed. Different options were compared considering model parameterization, numerical implementation and inversion. Proposals were made for establishing bridges between efficiency, friction force and suppliers' data, in particular for the identification of model structure and parameters.

Work is now in progress to implement more generic friction models with an object-oriented view. It is intended, in particular, to reproduce the influence of preloading in mechanical power transformers and the influence of external loads on bearings and joints. Modelling failures and enabling failure injection, linking the friction model to compliance/backlash, are also of prime interest to make friction models more realistic.

Declaration of conflicting interests

The author declares that there is no conflict of interest.

Funding

This research received no specific grant from any funding agency in the public, commercial or not-for-profit sectors.

References

1. Maré J-C. Historical evolution and challenges in aerospace. In: *Electronic proceedings of Actuator 2012,13th international conference on new actuators*, Bremen, 18–20 June 2012.
2. Todeschi M. Airbus – EMAs for flight controls actuation system: 2012 status and perspectives. In: *Proceedings of the 5th international conference on recent advances in aerospace actuation systems and components*, INSA Toulouse, Toulouse, 13–14 June 2012, pp.1–10. Toulouse: INSA
3. Maré J-C. Friction modelling and simulation at system level: a practical view for the designer. *Proc IMechE, Part I: J Systems and Control Engineering* 2012; 226(6): 728–741.
4. Karam W and Maré J-C. Force control of a roller-screw electro-mechanical actuator for dynamic loading of aerospace actuators. In: *Proceedings of the Bath/ASME symposium on fluid power and motion control*, Bath, 10–12 September 2008. Basildon: Harness Publicity LTD.
5. Hospital F. *Conception préliminaire des actionneurs électromécaniques basée sur les modèles. Lois d'estimation et règles de concepton pour la transmission de puissance mécanique*. PhD Dissertation, Institut National des Sciences Appliquées de Toulouse, Toulouse, 2012.
6. Stavytsky V, Nosko P, Fil P, et al. Load independent power losses of gear systems: a review. *TEKA Kom Mot i Energ Roln – OL PAN* 2010; 10B: 205–213.
7. Seetharaman S. *Investigation of load independent power losses of gear*. PhD Dissertation, The Ohio State University, Columbus, OH, 2009.
8. Croes J and Iqbal S. *Literature survey: gear losses*. Deliverable 2.1 of energy software tools for sustainable machine design, European Community Strep 247982, 2011, 22 pp., http://www.estomad.org/
9. Dudley DW and Townsend P. *Dudley's gear handbook*. New York: McGraw-Hill, 1991.
10. Pleguezuelos M, Pedrero J and Sánchez M. Analytical expression of the efficiency of involute spur gears. In: *13th World congress in mechanism and machine science*, Guanajuato, México, 19–25 June 2011, paper no. A9_558, pp.1–9.
11. Kohara Gear Industry. Practical information on gears, http://www.khkgears.co.jp
12. Anderson NE and Loewenthal SH. Design of spur gears for improved efficiency. *ASME J Mech Des: T ASME* 1982; 104: 767–774.
13. Dohring ME, Lee E and Newman WS. A load dependent transmission friction model: theory and experiments. In: *Proceedings of the IEEE international conference on robotics and automation*, Atlanta, GA, 2–6 May 1993, vol. 3, pp.430–436. New York: IEEE.
14. Misharin JA. Influence of the friction condition on the magnitude of the friction coefficient in the case of rolling with sliding. In: *Proceedings of international conference on gearing 1958 institute of mechanical engineers*, London, 23–25 September 1958, pp.159–164.
15. Benedict GH and Kelley BW. Instantaneous coefficients of gear tooth friction. *Tribol T* 1961; 4: 59–70.
16. O'Donoghue JP and Cameron A. Friction and temperature in rolling sliding contacts. *ASLE Trans* 1966; 9: 186–194.
17. Drozdov YN and Gavrikov YA. Friction and scoring under the conditions of simultaneous rolling and sliding of bodies. *Wear* 1968; 11: 291–302.
18. ISO/TR 13989. Calculation of scuffing load capacity of cylindrical, bevel and hypoid gears, 2007.
19. Neale MJ. *The tribology handbook*. 2nd ed. Butterworth-Heinemann, 1995.
20. Höhn B, Michaelis K and Döbereiner R. Load carrying capacity properties of fast biodegradable gear lubricants. *J STLE Lubr Eng* 1999; 55(11): 15–36.
21. Lundberg G and Palmgren A. *Dynamic capacity of rolling bearings* (Acta Polytechnica, Mechanical Engineering Series, vol. 1, no. 3). Stockholm: Royal Swedish Academy of Engineering Sciences, 1947.
22. The SKF model for calculating the frictional moment, http://www.skf.com
23. Starting and running torques. Technical report, http://www.nsk.com
24. Technical description of ball screws. *NSK Tech J*, http://www.nsk.com
25. Vis à billes, SKF technical publication 4141 FR, December 2006. Gothenburg: SKF.
26. *Nook planetary roller screws* (Nook technical catalogue), http://www.nookindustries.com/Product/ProductLine/Planetary-Roller-Screw-Products

27. Vis à rouleaux satellites Rollvis (Rollvis technical catalogue), http://www.elitec-tl.com/index.php/Vis-d-entrainement/Vis-a-rouleaux-satellites-Rollvis.html
28. Roller screws, SKF technical publication 4351 EN, June 2005. Gothenburg: SKF.
29. Wittenstein products, http://www.wittenstein-alpha.de (2009).
30. Fine Cyclo complete catalogue, http://www.sumito modriveeurope.com
31. Spinea Twin Spin® catalogue, http://www.spinea.sk
32. Harmonic Drive AG 2008 catalogue, http://www.harmonicdrive.de
33. Herrera C, Gorla B and Maré J-C. Towards adaptive control of a positioning electrohydraulic actuator. *Journal of Automation and Computer Integrated Manufacturing* 1991; 4(2): 123–140.
34. Koskinen EK, Saarinen H and Tuokko RO. Mechanics of seals friction with special reference to hydraulic cylinders applications. In: *Proceedings of the third Scandinavian international conference on fluid power*, Tampere, 25–26 May 1993, pp.381–401. Tampere: Tampere University of Technology.
35. Wartelle M. Modèles mathématiques des organes hydrauliques. *Bulletin Cetim* 1978; 4–17.
36. Bonchis A, Corke PI and Rye DC. A pressure-based velocity independent, friction model for asymmetric hydraulic cylinders. In: *Proceedings of the IEEE international conference on robotics and automation*, Detroit, MI, May 1999, pp.1746–1751. New York: IEEE.
37. Kuhnlein M, Murrenhoff H, Dombrowski RV et al. Rapid parameterisation of a sealing friction model for hydraulic cylinders. In: *Proceedings of the 8th international fluid power conference*, Dresden, 26–28 March 2012, vol. 1, pp. 333–344.
38. Wang L. *Force equalization for active/active redundant actuation system involving servo-hydraulic and electromechanical technologies*. PhD Dissertation, INSA Toulouse, Toulouse, 18 December 2012., vol 1, pp. 333–344.
39. Canudas de Wit C, Olsson H, Åström KJ, et al. A new model for control of systems with friction. *IEEE T Automat Contr* 1995; 40(3): 419–425.
40. Bo Tran X and Yanada H. Modeling of dynamic friction behaviours of fluid power actuators. In: *Electronic proceedings of the 12th Scandinavian international conference on fluid power*, Tampere, 18–20 May 2011. Tampere: Tampere University of Technology.
41. Ivantysyn J and Ivantysynova M. *Hydrostatic pumps and motors*. New Delhi, India: Akademia Book International, 2001.
42. Maré J-C. System level modelling of mechanical losses in actuators. In: *Proceedings of the 20th international conference on hydraulics and pneumatics*, Prague, 29 September–1 October 2008. Ostrava: Czech Mechanical Engineering Society, Technical University of Ostrava.
43. Martineau J-P, Chedmail P. Caractérisation expérimentale et modélisation du comportement des réducteurs Harmonic Drive. In: *4th World congress on gearing and power transmission*, Paris, 16–18 March 1999, pp.1089–1100. Paris: MCI.
44. Karam W and Maré J-C. Modelling and simulation of mechanical transmission in roller-screw electromechanical actuators. *Aircr Eng Aerosp Tec* 2009; 81(4): 288–298.
45. Iordanidis G, Grac S, Maré J-C, et al. An overview of modelling and simulation activities for an all-electric nose wheel steering system. In: *Proceedings of the 4th international conference on recent advances in aerospace actuation systems and components*, INSA Toulouse, Toulouse, 5–7 May 2010, pp.137–145.
46. Hamon P, Gautier M and Garrec P. New dry friction model with load and velocity dependence and dynamic identification of multi-DOF robots. In: *Proceedings of IEEE international conference on robotics and automation*, Shanghai, China, 9–13 May 2011, pp.1077–1084. New York: IEEE.
47. Jansen L, Hölscher H, Fuchs H, et al. Temperature dependence of atomic scale stick-slip friction. *Phys Rev Lett* 2010; 104: 256101-1–256101-4.
48. Gruebler R and Hora P. Temperature dependent friction modelling for sheet metal forming. *Int J Mater Form* 2009; 2: 251–254.
49. Li JW, Chen XB, An Q, et al. Friction models incorporating thermal effects in highly precision actuators. *Rev Sci Instrum* 2009; 80: 045104-1–045104-6.
50. Bittencourt AC, Wernholt E, Sander-Tavallaey S, et al. An extended friction model to capture load and temperature effects in robot joints. In: *IEEE/RSJ international conference on intelligent robots and systems*, Tapei, Taiwan, 18–22 October 2010, pp.6161–6167. New York: IEEE.
51. Karnopp D. Computer simulation of stick slip friction in mechanical dynamic systems. *J Dyn Syst: T ASME* 1985; 107(1): 100–103.
52. Otter M, Elmqvist H and Mattson SE. Hybrid modelling in Modelica based on the synchronous data flow principle. In: *IEEE symposium on computer-aided control system design*, Kohala Coast, HI, 22–27 August 1999, pp.151–157. New York: IEEE.
53. Nfonguem G and Maré J-C. Inverse simulation of an aerospace redundant electro-hydraulic actuator. In: *Proceedings of the sixth international conference of fluid power transmission and control*, Hangzhou, China, 6–8 April 2005, pp.518–521. International Academic Publishers-World publishing corporation.
54. Pelchen C, Schweiger C and Otter M. Modelling and simulation of the efficiency in gearboxes and planetary gearboxes. In: *Proceedings of the second international Modelica conference*, Oberpfaffenhofen, 18–19 March 2002, pp.257–266. Germany: The Modelica Association.

Appendix I

Notation

a	friction model parameter or center distance
c	general friction parameter
C_0	static load rating
d, D	diameter (pinion/gear)
f	bearing type–dependent factor
f	viscous friction coefficient
F	force
h	lubricant film thickness
H_s, H_t	specific sliding at approach and recess
I_{rm}	polynomial friction factor
k	sliding friction coefficient
m	module
M	mass
n	shape factor

p	pitch
P	pressure
R	reduction ratio
Ra	roughness (quadratic mean)
s	lubrication quality parameter
S	entropy
SN	service number
t	time
T	torque
V	translational velocity
z	mean deflection of contact asperities
z, Z	number of teeth
α	pressure angle
β	helix angle
γ	reference cylinder lead angle
ε_α	transverse contact ratio
ζ	relative fluid film thickness
η	mechanical efficiency
Θ	temperature
μ	friction coefficient
μ	dynamic viscosity
σ_0	stiffness of contact bristles
σ_2	viscous friction factor
τ	time constant
φ	friction angle
ω	angular velocity

Subscripts/superscripts

a	outside
b	base
C	Coulomb
d	direct
D	drive
e	equivalent
E	external
g	geometry
i	indirect
l	liquid
L	load
m	mean
M	mobile
n	normal
N	normal
o	outside
p	preload, pseudo
P	pressure
r	relative
R	reference, rated
s	solid
S	Stribeck
x	axial
w	worm
Δ	difference
0	rolling, no-load
1	sliding
∞	limit value
Θ	temperature